TAILOR SYNTHESIS OF INORGANIC NANOSTRUCTURES FOR DIRECT INTEGRATION INTO SOLAR CELLS

A Senior Scholars Thesis

by

Maxime Van Laer

Submitted to Honors and Undergraduate Research
Texas A&M University
in partial fulfillment of the requirements for the designation as

UNDERGRADUATE RESEARCH SCHOLAR

May 2012

Major: Chemical Engineering

TAILOR SYNTHESIS OF INORGANIC NANOSTRUCTURES FOR DIRECT INTEGRATION INTO SOLAR CELLS

A Senior Scholars Thesis

by

Maxime Van Laer

Submitted to Honors and Undergraduate Research
Texas A&M University
in partial fulfillment of the requirements for the designation as

UNDERGRADUATE RESEARCH SCHOLAR

Approved by:

Research Advisor: Sreeram Vaddiraju
Associate Director, Honors and Undergraduate Research: Duncan MacKenzie

May 2012

Major: Chemical Engineering

ABSTRACT

Tailor Synthesis of Inorganic Nanostructures for Direct Integration into Solar Cells.
(May 2012)

Maxime Van Laer
Department of Chemical Engineering
Texas A&M University

Research Advisor: Dr. Sreeram Vaddiraju
Department of Chemical Engineering

The fundamental aim of this project is the synthesis of inorganic compound semiconductor nanowires using chemical vapor deposition (CVD). More specifically, use of zinc and phosphorus for the self catalytic synthesis of Zn_3P_2 nanowires is studied in detail in this work. The effect of process parameters on nanowire formation is also comprehensively investigated. This study allowed for the scaling of nanowire production, amplifying the process to yield gram quantities.

It is essential to emphasize here that large scale synthesis of nanowire powders is useful for the manufacture of a renewable energy conversion device, such as solar cells. Nanowire properties enhance solar cell performance by increasing the capacity of a photoabsorbing material, through an increase in surface area available for absorption. This project aims to produce such materials, of high purity, and of high stability, while maintaining enhanced electrical and optical properties.

ACKNOWLEDGEMENTS

Maxime Van Laer would like to acknowledge Dr. Sreeram Vaddiraju for providing this opportunity of self development. The author also expresses gratitude to Lance Brockway, Yongmin Kang, and Venkata Vasiraju for their support. This project was partially funded by the National Science Foundation and the Department of Energy.

NOMENCLATURE

CVD	Chemical Vapor Deposition
MCF	Materials Characterization Facility
Zn_3P_2	Zinc Phosphide
Sccm	Standard Cubic Centimeter per Minute
XRD	X-ray Diffraction
SEM	Scanning Electron Mictroscope/y
TEM	Tunneling Electron Microscope/y
XPS	X-ray Photoelectron Spectroscopy
UV-Vis	Ultraviolet Visible Spectroscopy
FTIR	Fourier Transform Infrared Spectroscopy
THF	Tetrahydrofuran
VLS	Vapor-Liquid-Solid

TABLE OF CONTENTS

Page

LIST OF FIGURES

CHAPTER I

INTRODUCTION

The problem

Fossil fuels dominate worldwide supply of energy, yet remain a non renewable source. Efforts to dilute the world's dependence on hydrocarbon fuel are pale, as fossil fuels currently represent 86.4% of the global energy consumption[1]. Still, alternative sources are becoming ever more prominent as hydroelectric power and nuclear power generate 6.3% and 8.5%, respectively[1], of the world's energy. By far the most promising alternative to fossil fuels remains solar power. One has to do little more than observe the mechanism employed by nature; as plants harvest the sun's light energy to break down water and reduce carbon dioxide into carbohydrates as a "usable" energy source[2]. A more applicable way the sun's light energy can be used to create fuel is through the excitation of electrons known as the photovoltaic effect. It has been postulated that if 0.1% of the earth's surface area were covered with 10% efficiency solar cells, the energy demands of the entire planet can be met[1]. Hence, one of the problems that needs to be addressed when looking to harvest solar energy is the large scale manufacturing of appropriate materials. The material manufactured also need to be inexpensive, abundant, and non toxic, if solar cells are to be an imposing provider for energy in the future.

This thesis follows the style of *Journal of The Royal Society of Chemistry*.

The inspiration

The problem posed above leads to a series of questions a scientist must address when considering the development of solar cells: which materials are viable absorbers of solar light, and how can they be manufactured on a large scale? The answer to the former question, and the cog which triggered this research project, came in the form of a potato chip bag. As unlikely a source of inspiration; the interior of a potato chip bag is lined with a uniform thin film of aluminum. The thin film is deposited through a physical vapor transport mechanism, where the deposited layer can be controlled to nano (10^-9m) thicknesses[3]. The capitalist driven industry has maximized its resource efficiency to minimize material cost. Following the example of the packaging companies, this research project aims at using chemical vapor deposition (CVD) techniques to bulk produce materials for use in solar cells.[4]

The fundamental question

The other question fundamental to the success of this project regards the material chosen. The principal property of any photo absorbing material is its band gap, as it defines what range of the solar spectrum the photovoltaic cell absorbs[5]. Energy of light is directly proportional to its frequency(υ) following De Broglie's equation E=υ*h where h is planck's constant[6]. In accordance with the photovoltaic effect, a valence electron, upon irradiation with sunlight, absorbs the photon's energy and gets excited to a higher energy level, which would be the conduction band. In a semiconductor the conduction band is separated from the valence band by an energy band gap. If the energy gap in the

material is high, the electrons won't be excited by low energy photons, while if the energy of photons is too high, the extra energy will be lost[5]. Therefore for an ideal solar cell material, the energy gap should match the energy of the incident photons (light).

The sun may be considered as a hot object due to its hydrogen fusion cycle, so, according to Rayleigh's theory of blackbody radiation, the radiation emitted by the sun is the same as that of a hot object[1]. The electromagnetic spectrum spans a wide range of wavelengths and a black body radiator emits all of them, with the relative percentage of each frequency (directly proportional to energy) depending on temperature. The composition emitted by sun, or a body at the equivalent temperature of 5800 K, is primarily composed of visible light, infrared and ultraviolet light[1]. However, our atmosphere also filters out specific sections of the electromagnetic spectrum. Water vapor and specifically ozone (O_3) have absorption bands in the UV region, causing only 0.5% of the total UV light to penetrate the atmosphere and reach the earth's surface. Visible light has an energy ranging from 1.71 to 3.1 eV for red and violet light respectively, while infrared radiation have an energy ranging from 0.01 to 1.71 eV. Accordingly, theoretical studies have shown that 1.5 eV is the best energy gap to achieve a maximum efficiency in a single junction photovoltaic cell[7].

Background

A 1.5 eV energy gap imposes strict constraints for many materials, as a larger or smaller band gap will waste the lower and higher frequencies of the incident radiation respectively. Silicon, which dominates worldwide sales of photovoltaic cells, has a band

gap of 1.1 eV, and for that reason is condemned to underperform. The search for materials to replace silicon has been propelled by modern advancements in nanotechnology. Nanotechnology allows for the accurate engineering of the bandgap, thus widening the number of materials which could be suitable photoabsorbers[8]. By changing the size of a material, the band gap can be increased. This is achieved by creating very small structures (10^{-9}m) where excitons, electron-hole pairs, can be quantum-confined. The band gap increase as a result of a decrease in the number of contributing atoms in the lattice. The lower the number of atoms, the less the number of contributing orbitals, thus breaking up the continuous energy states from the superimposing orbitals; or in other words quantumly confining the electrons[9]. The manipulation of such electrical properties grants one a freedom that extends beyond silicon, the current standard[10], when choosing the materials necessary to develop solar technology.

The material chosen for this work is zinc phosphide (Zn_3P_2). Partly for its ideal electrical properties, as its band gap of 1.39eV[11] is close to the ideal value for a photoabsorbing material of 1.5eV[12], and partly for its wide availability (Zinc Phosphide is frequently employed as rat poison). Additionally, nanowire morphology is chosen which would allow a macroscopic dimension to remain (the length). In a nanowire structure, exciton pairs are confined in the radial dimension (r and θ), while bulk properties remain in the length (z) direction, where electrical charge may pass unconstrained[13]. Surface area to volume ratio also increases as radius decreases[14], shown geometrically below for

nanowires approximated as cylinders, which allows for nanowires to absorb more incident radiation due to the increase in surface for contact.

$$A_{end} = pi*r\text{^}2$$

$$A_{surface} = 2pi*r*h$$

$$A_{total} = A_{surface} + 2*A_{end}$$

$$V = A_{end}*h$$

$$\rightarrow A/V = 2(r+h)/rh$$

Surface passivation

Metals have delocalized valence electrons due their outer orbital extending over several adjacent atoms[15] (which is what grants them favorable electrical properties), but it also means the ionization energy to remove an electron from a metal atom is very low (low electron affinity); in other words metals oxidize easily. Due to the bond between a metal and nonmetal, metal oxides are ionic in character[16] (ceramic), resulting in very stable molecules (high energy bonds) with high boiling and melting points. Zinc is no exception, being a transition metal with a valence configuration of $4s^2\ 3d^{10}$; zinc readily forms zinc oxide[17] (ZnO) even at room temperatures. The ZnO bond is largely ionic in character according to Pauling (difference in electronegativity), with a value of 1.79 (>2 means fully ionic). Zinc oxide begins to melt in atmospheric pressure at around 2000 C, well above that of pure zinc (420 C)[18]. Additionally, the morphology of the deposited surface also affects its stability. As previously metioned, the surface area to volume ratio increases as radius decreases. This increase in surface for nanowires provides more

contact space with external molecules, which leads to an increase in reactivity since the number of possible reaction sites has increased[19]. With these considerations in mind, the fabrication of any metal nanomaterial would be incomplete without proper surface stabilization methods.

CHAPTER II

METHOD

Reactive vapor transport

Zn_3P_2 nanowires were made using Chemical Vapor Deposition (CVD). In CVD, volatile (high vapor pressure) precursors serve as the source of the material. The gas precursors diffuse though the reactor and adsorb on the deposition surface. This is followed by a reaction of the adsorbed species leading to the formation of the desired species[20]. Choice of precursor also depends on the ease with which it reacts. For example ammonia (NH3) is often used to provide nitrogen rather than regular N2 gas. The N2 bond is a triple bond and very strong, hence the resolve to use ammonia[21]. Many precursors need to adsorb on a highly reactive surface to crack into their constituents, and this necessity often results in the need of a catalyst[22].

Due to phosphorous high vapor pressure[23], the direct use of pure phosphorous as a source material can be used, without the need of a precursor or catalyst. This simplifies the mechanism since no reactive cracking at the catalyst surface needs to occur; therefore the mechanism employed is correctly defined as reactive vapor transport.

Although catalytic substrates can be used[24], circumventilating the use of an impurity catalyst is of drastic importance since these impurities would otherwise alter the properties of the nanowires. Any foreign atom affects the band gap of a material by imposing its own energy levels, changing the electrical properties[25]. Additionally, the

one dimensional anistropy of the nanowires means that any electrical current has to pass through the same coherent volume along the length[14]. Therefore the presence of a single impurity would potentially thwart the electrical properties of the entire wire. Hence the ability to grow nanowires is a pure form without the presence of catalyst contamination is a critically important.

Thermodynamics

The mechanism leading to the formation of nanowires is known as VLS or vapor-liquid-solid. A vapor of phosphorous comes into contact and adsorbs on the surface of the liquid zinc droplets, diffusing within them. Once the saturation levels are exceeded, zinc phosphide crystal is precipitated from the droplet at the solid liquid interface with the substrate[26]. This phase transition coins the terminology vapor-liquid-solid, which fashions a self growing wire from its own tip.

The fundamental driving force of the nanowire formation is driven by the partial pressure of phosphorous, and its solubility in zinc[27] (around 1% at the lowest temperature where the liquid alloy is formed). The zinc substrate is located at the cooler end of the gradient, where temperatures are set just high enough with respect to the melting point of pure zinc that liquid droplets of the material form on the surface. This is envisioned in the zinc phosphorous phase diagram with pure zinc shown at the right extremity of the diagram melting at 420 C. Since only slight melting is desired, the

substrate temperature was set only to 405C. Molecules on the surface of solids have more energy compared to the bulk of the material[28] (otherwise all material bodies would have a natural tendency to sublime) and are intrinsically less energetically favored. This explains why melting always occurs first at the surface.

The lowest temperature where phosphorous and zinc form a binary liquid mixture is marked by the eutectic temperature at 420 C and 1% phosphorous concentrations[29].

Raising the phosphorous pressure in the reactor will force the concentration of phosphorous within the binary liquid to surpass equilibrium concentrations, and push the system past the phase boundary. The partial pressure difference acts as a driving force for the supersaturation of the droplet, where the two components can no longer coexist as a single phase and the precipitation of Zn3P2 solid arises. It is important to notice the relatively low P concentration at the eutectic point[29], signifying low P solubility in Zn. The low solubility means that the energy cost of increasing the P concentration beyond its equilibrium value will be high. This is also shown by the steep equilibrium line where a large increase in temperature (energy) only results in a slight increase in solubility. It is also noted that the solubility of P in Zn remain low until temperatures of over 800 C[29]. This means that to enable efficient growth, a high flux of phosphorous must be provided, otherwise nanowire growth will be slow. This can be achieved by raising the phosphorous source temperature, which will result in phosphorous saturation within the reactor in the vapor phase, and raise P partial pressure.

Process

In this experiment, the reactants were phosphorous and zinc, with the phosphorous being vapor transported onto zinc. The reactor was maintained in vacuum to prevent oxidation, with hydrogen acting as a carrier gas to aid the transport of phosphorous. The reactor is a hot-walled chamber composed of a quartz tube housed inside a three-zone oven, in which a temperature gradient could be programmed. The gradient was made possible by the manipulation of three thermocouples integrated in a loop which constantly measure and readjust power accordingly, resulting in very accurate temperatures. The quartz tube was connected to mass flow controllers to regulate flow of the carrier gas, a pressure-transducer for the measurement of the reactor pressure, and a vacuum pump with a carbon filter (to filter the outlet air leaving the pump). Quartz was used because of its extremely high melting point[19] and stability (inert), which prevents it from contaminating the reaction. A silica ceramic covers the ends of the tubular reactor, and serves as thermal insulation. The inlet is connected to a piping system where a hydrogen gas cylinder and a small reservoir (bubbler) are connected in parallel. This allows for organic molecules to be introduced into the process via the reservoir without outside exposure. Surface stability of the zinc phosphide nanowires will be achieved through a coating with a monolayer of organic molecules. The organics will be introduced within the reactor in the vapor phase after synthesis, in an *insitu* fashion, to prevent exposure to oxygen at any point in the process. Thiol functional groups will be used to bond the organic molecules to the surface of zinc phosphide by bonding with the dangling metal zinc bonds[30]. The saturation of these dangling bonds will prevent them

from undergoing oxidation, and shield the wires. A schematic of the reactor setup can be seen in Figure 1.

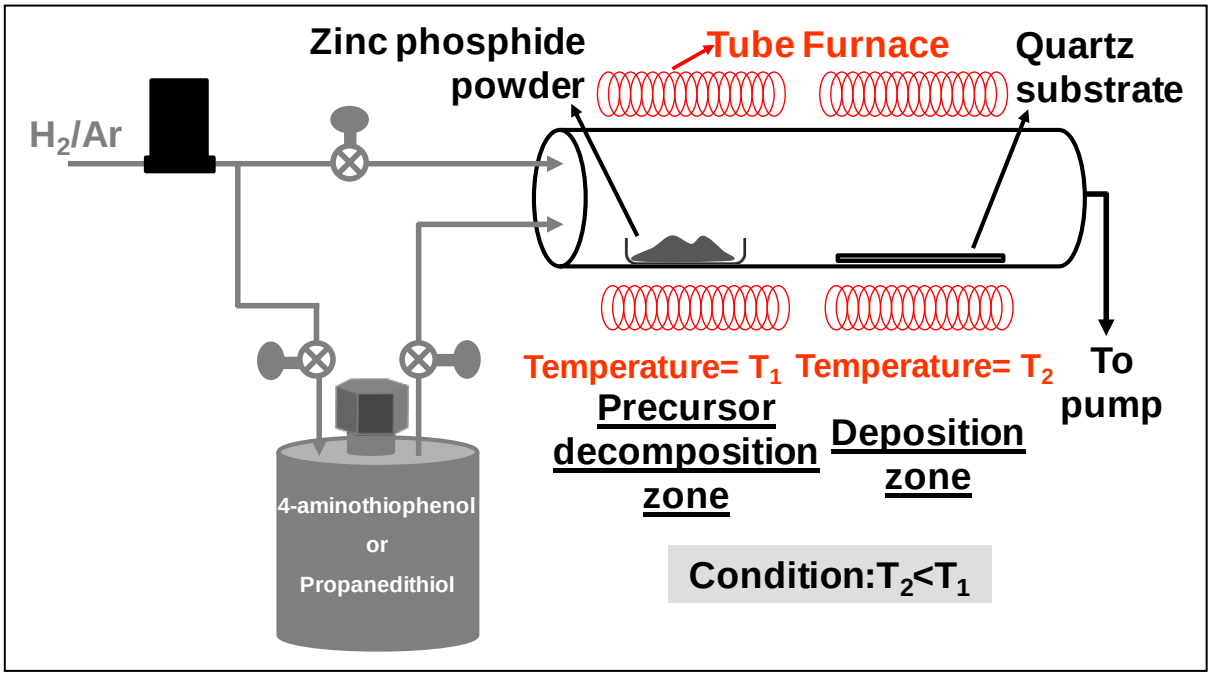

Figure 1. Schematic of the multi-zone tube furnace

Procedure

Firstly, a boron nitride crucible is used to hold 50 mg of red phosphorus at the hot end of the reactor, which is maintained at a temperature of 480°C. The zinc substrates were coiled into foils of 2.5cm in diameter, and placed downstream at a temperature of 405°C. A flow of 20 sccm of hydrogen gas maintains a pressure of 2 Torr. The zinc substrates were prepared by submersion in a solution of 25 ml 98% hydrochloric acid, and 25ml de ionized water. The substrates were kept in solution for 30 seconds to remove any

preexisting metal oxide layer. Upon removal from the acid solution, residue acid was washed off thoroughly with first water and then acetone.

In-situ functionalization of the synthesized Zn_3P_2 nanowires was accomplished after the synthesis by re-routing the hydrogen flow through the bubbler, exposing the nanowires to a vapor of the organic molecule 4-aminothiophenol. The bubbler holding the functional molecules was heated to a temperature of 110^{o}C, enough to vaporize a solid source of the organic[31]. For functionalization, tube reactor temperature and thus substrate temperature were cooled to 100 ^{o}C (The zinc sulfur bond forms at around 80 ^{o}C[32]), to halt the flux of phosphorous, and prevent the organic molecule from decomposing. The resultant products were characterized using SEM, XRD, TEM and FTIR.

CHAPTER III

RESULTS

Material characterization

The reactive vapor transport experiments lead to the formation of green/yellow deposit. The green deposit is confirmed to be composed of nanowires by SEM microscopy, with an average diameter of 25-40 nm and several tens of microns long, as shown in Figure 2(a). Phase and composition of the wires was verified by XRD analysis, indicating α-Zn_3P_2 composition as expected with the phase diagram. Zinc phosphide has a tetragonal crystal structure, which is shown in crystallographic x-ray spectroscopy by comparison with the original zinc phosphide source material Figure(b). The Zn_3P_2 nanowires are single crystalline with a growth direction of [131] as shown by TEM analysis of the nanowires. The amount of nanowire powder obtained using the method of quartz substrate deposition was very small, 2-3 milligrams per run. The majority of the source was observed to deposit elsewhere along the tube, representing large resource inefficiencies.

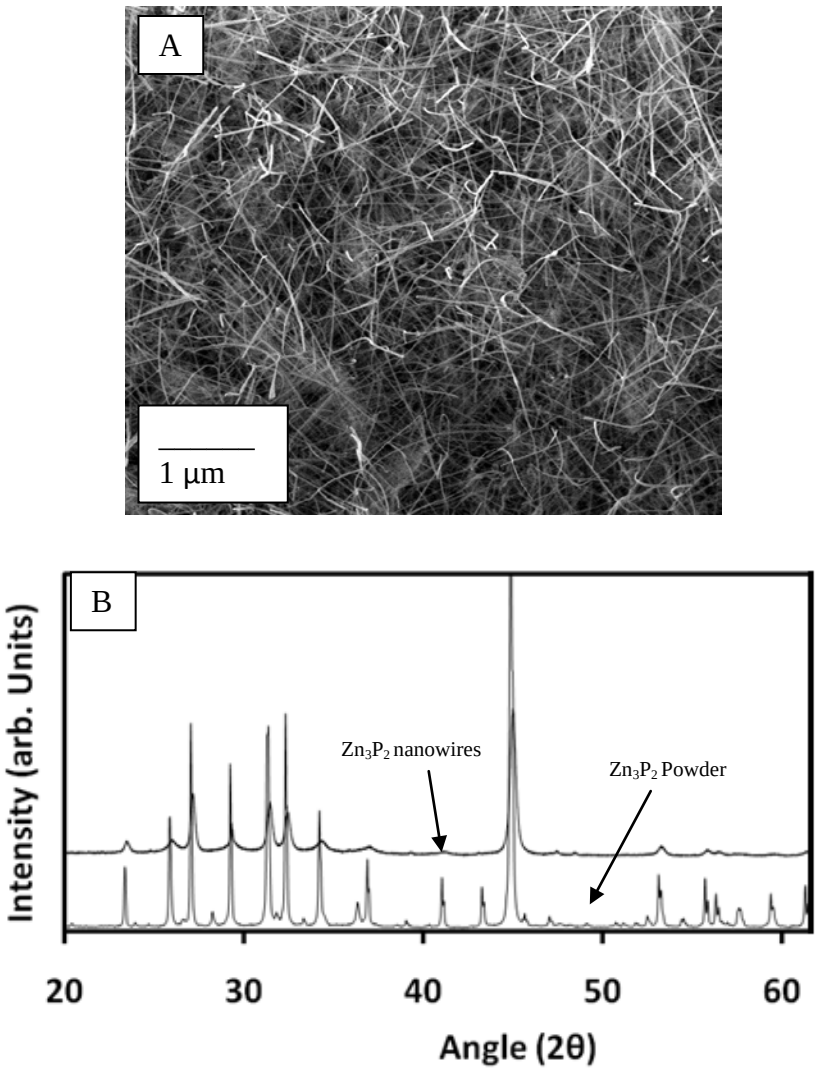

Figure 2. (a) SEM and (b) XRD of nanowires on quartz substrates

Thiolation stability enhancement

As observed in Figure 3(a), no changes in the morphology or structure of the nanowires were observed after their *in-situ* functionalization. The images in Figure 3 represent the stability enhancement tests performed on the nanowires. SEM images of the nanowires were taken after 120 days in a solution of THF. The vapor functionalized nanowires,

shown in Figure 3(a), exhibit no signs of agglomeration or surface degradation. The unfunctionalized Zn_3P_2 nanowires, Figure 3(b), show clear regression of quality, as symptoms of surface degradation and agglomeration are clearly visible.

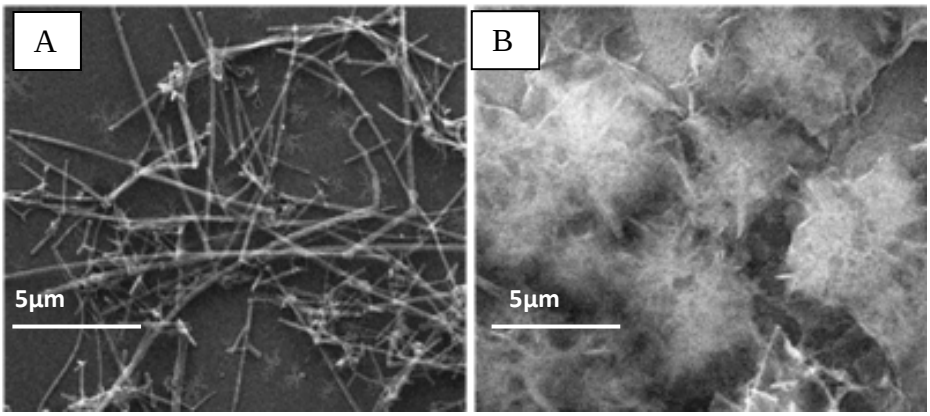

Figure 3. SEM images of (a) functionalized and (b) unfunctionalized nanowires

Zn_3P_2 nanowire surface analysis

To confirm the success in bonding the organic molecule with the zinc phosphide surface, Fourier Transform Infrared Spectroscopy (FTIR) is used to detect the rotational-vibrational identity of the bonds formed by the molecule. The characteristics of a molecule are determined by its bonding and the electronic hybridization of its orbitals[33], where the states an electron may assume within a molecule are called its quantum mechanical states. Radiation is most probable to be absorbed at frequencies that are similar to the energy difference between two of those quantum mechanical states[34].

The absorption that occurs from this transition between states is displayed as an absorption line on spectroscophic graphs such as Figure 4, where each line derives directly from the bonding between two atoms in the molecule.

The formation of Zn-S bonds between the 4-ATP organic molecules and the Zn_3P_2 nanowire surfaces does not absorb frequencies within the infrared spectrum range[35] (it lies at the very bottom of the fingerprint range where the lowest energy bonds within the IR spectrum lie). However the sulfur hydrogen (S-H) thiol peak is present at around 2550 wavenumbers (λ^{-1}). The disappearance of the S-H bond would indicate the formation of new sulfur bonds with the zinc surface. In the thiolation chemistry employed, the sulfur of the 4-ATP favorably forms covalent bonds with zinc atoms[32]. This deprotonation of sulfur with the disappearance of the thiol peak is shown in Figure (4), where the functionalized sample, represented by the top line, has no peak at 2550 cm^{-1}. This is further indicative of the isolation of thiol reactions to zinc atoms alone, since the amine stretch at 3300 cm^{-1} remains untouched. The only bonding change is therefore observed between the dangling surface zinc atoms and the sulfur functional group. These form a thiolate, while preserving the structure and integrity of the system.

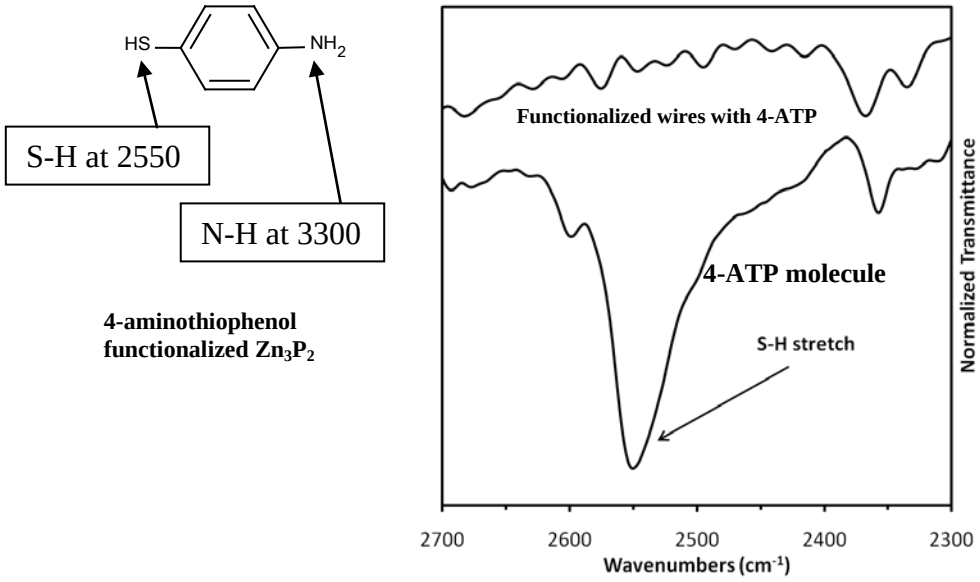

Figure 4. FTIR spectrograph of functionalized ATP nanowires

Scale up to bulk production

To accomplish the bulk synthesis of gram quantities of nanowire powders, an adjustment was made by having pure phosphorus transported in the vapor phase directly onto heated zinc foils. The introduction of zinc as a deposition surface not only provides an almost unlimited source of material, but also the additional convenience of removing the need for a substrate. The constraints on the quantity output are thus reduced to the reaction time and, to a large extent, the amount of phosphorous. Consequently, to further optimize the quantity produced per time, the area over which the nanowires can be obtained is maximized by taking advantage of zinc's malleable characteristics[36]. The foil dimensions are increased to 30 x 8 cm^2 and fit concentrically into the 1 inch diameter tube reactor. This results in a 955% increase to the maximum surface area allowed per length, which otherwise would be the tube circumference. If one considers that the

incorporation of such a model allows for deposition of nanowires on both faces of the zinc substrate, surface area increases are nearly double at 1910%. Owing to the high thermal conductivity of zinc metal[37], no appreciable thermal gradients are expected across the length of the foil, and the entire foil is considered to be isothermal under the experimental conditions.

Vapor transport of phosphorus onto zinc foil was successful in the formation of Zn_3P_2 nanowires. Figures 5(a) are photographs of the zinc substrate after synthesis, with deposit uniformly formed on both sides. SEM analysis of the deposit verifies the presence of Zn_3P_2 nanowires 20-40 nm in diameter as shown in Figure 5(b). The density of the Zn_3P_2 nanowires on the surface of the zinc foil was calculated to be roughly $10^9/cm^2$. Zn_3P_2 nanowire powder was obtained by scraping the foils using a razor blade and collecting pristine nanowires in jars packed under argon (a inert gas) as shown in Figure 5(c). On average, 1.5 to 2 grams of nanowire powder was produced per run.

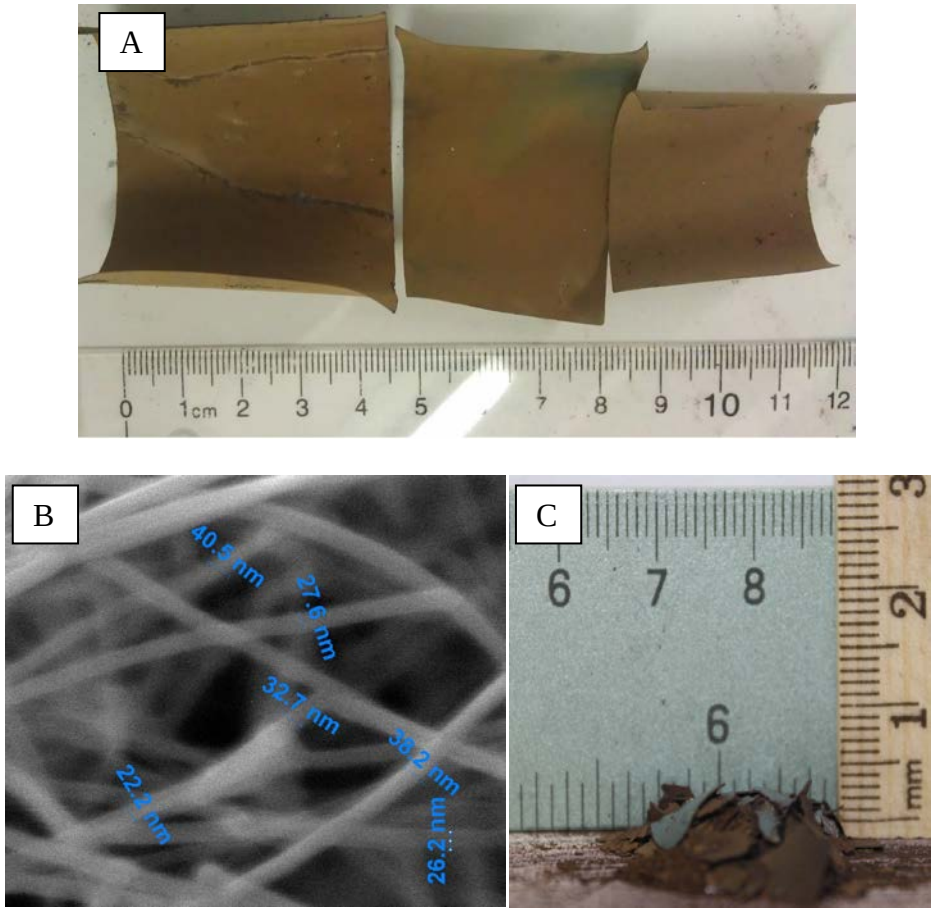

Figure 5. (a), (c) optical photograph and (b) SEM of large quantity nanowire powders

Mechanism

Premature experiments of a total duration of five minutes were performed to understand the formative mechanism responsible for nanowire growth. According to these short-term experiments, the formation of Zn_3P_2 crystal nuclei on the surface of the foils is observed as a precedent to nanowire growth. The nanowires are then found to selectively grow on the surface on these Zn_3P_2 crystals. This spontaneous phenomena is a clear characteristic of self catalysis, a mechanism in which the source material (in this case

zinc) fuels and stimulates its own growth[38]. The Zn_3P_2 self catalysis, like all other vapor-liquid-solid mechanisms, occurs because of the relative surface energies[39]. Zn_3P_2 crystals significantly raise surface energy of the substrate and hence cause the melted zinc droplets to selectively form only on their surface alone due to the creation of higher energy, and hence more stable bonds. In turn the surface energy of the zinc droplets relative to the crystals is low, representing a favor in zinc cohesion over surface adhesion to the crystals. This is observed by the formation of a spherical droplet as noticed in Figure 2(a). Further phosphorous flux leads to phosphorus adsorption from the vapor phase to the surface of the liquid droplet which in turn diffuses and supersaturates the droplet. Upon reaching saturation levels of phosphorus, zinc phosphide is precipitated as a solid crystal from the liquid-crystal interface, resulting in the one-dimensional growth of nanowires. To further optimize the growth mechanism, settings must be adjusted relative to the material. The melting point of zinc, originally at 420 C, increases with doping concentration of phosphorous through vapor solid adsorption[40]. These colligative properties raise the melting point of zinc, which lowers the amount of zinc provided in the vapor phase. Therefore as the concentration of phosphorous in the zinc from solid state diffusion increases, so should the temperature of the reactor be increased. Failure to do so would result in the termination of zinc flux in the vapor phase, preventing further wire growth once the zinc liquid droplet depletes. In essence, the zinc foils served not only as the substrates but also as the source in the Zn_3P_2 nanowire formation.

CHAPTER IV

SUMMARY

Conclusion

Nanotechnology has been shown to alter electrical, optical, and magnetic properties of materials relative to their bulk counterparts[41]. This nano-phenomena opens the possibility of employing new materials, previously considered unfit, to be used in the manufacturing of energy conversion devices such as thermoelectrics or solar cells. Analysis of literature reveals many discovered material systems and enhanced properties[42-44], however, few of these methods report production on any significant scale. In order for the transition and integration of nanomaterials in real world applications and devices, methods to produce such materials in large quantities are crucial.

This thesis presents a material system, which, while maintaining enhanced nano-scale properties, is scalable to commercial levels to produce microscopic material in macroscopic quantities. The zinc phosphide nano wires produced are of coherent purity with no contaminants detected by any conventional characterization methods at our disposal. Surface Stabilization techniques employed to tame surface reactivity were shown to successfully prevent degradation of the nano wires in conditions similar to those of our outside environment. In conclusion the wires are produced from cheap source materials, are of high purity, and are stable. These versatile but nonetheless

critical components of this project yield a material suitable for immediate commercial integration in cheap high efficiency solar cells.

Final remarks

Large Scale production of Zinc phosphide nanowires was achieved by the vapor transport of phosphorous onto zinc foils. In-situ vapor phase stabilization of Zn_3P_2 nanowires using thiol chemistry to bond metals with organic molecules proved to protect the surface from oxidation and prevent their agglomeration. This technique proves to be efficient and consistent in execution, preventing formation of the dreaded oxide layer that haunts all metals from forming on the nanowires surface. The prevention of such oxide layer enables more organics to bond to the clean surface and removes the need for chemical etching which could, in turn, negatively degrade the size, morphology, and composition of the nanowires[45]. This large scale production and in-situ functionalization technique opens many opportunities for the development of stable nanomaterials. Furthermore, this material system provides fundamental information to help understand the properties and growth mechanisms controlling the nanowire parameters, so that nanosystems may be better comprehended.

REFERENCES

1. G. W. Crabtree and N. S. Lewis, *Physics Today*, 2007, **60**, 37-42.

2. K. R. Catchpole, *Philosophical Transactions of the Royal Society a-Mathematical Physical and Engineering Sciences*, 2006, **364**, 3493-3503.

3. H. O. Pierson and Knovel (Firm), in *Materials science and process technology series. Electronic materials and process technology*, Noyes Publications, Norwich, N.Y., 2nd edn., 1999.

4. S. Vaddiraju, University of Louisville, 2006, p. 158-176.

5. T. Zdanowicz, T. Rodziewicz and M. Zabkowska-Waclawek, *Solar Energy Materials and Solar Cells*, 2005, **87**, 757-769.

6. T. Trindade, P. O'Brien and N. L. Pickett, *Chemistry of Materials*, 2001, **13**, 3843-3858.

7. Y. Huang, X. F. Duan and C. M. Lieber, *Small*, 2005, **1**, 142-147.

8. T. Hanrath and B. A. Korgel, in *Physical Chemistry of Interfaces and Nanomaterials Iii*, eds. G. V. Hartland and X. Y. Zhu, 2004, vol. 5513, pp. 40-47.

9. K. F. Lin, H. M. Cheng, H. C. Hsu and W. F. Hsieh, *Applied Physics Letters*, 2006, **88**, 263117.

10. E. C. Garnett and P. D. Yang, *Journal of the American Chemical Society*, 2008, **130**, 9224-9225.

11. R. S. Yang, Y. L. Chueh, J. R. Morber, R. Snyder, L. J. Chou and Z. L. Wang, *Nano Letters*, 2007, **7**, 269-275.

12. A. Al-Azzawi, *Photonics : principles and practices*, CRC Press, Boca Raton, FL, 2007.

13. L. Zhang, X. Fang and C. Ye, *Controlled growth of nanomaterials*, World Scientific Pub., Hackensack, NJ, 2007.

14. R. Agarwal and C. M. Lieber, *Applied Physics a-Materials Science & Processing*, 2006, **85**, 209-215.

15. J. E. Allen, E. R. Hemesath, D. E. Perea, J. L. Lensch-Falk, Z. Y. Li, F. Yin, M. H. Gass, P. Wang, A. L. Bleloch, R. E. Palmer and L. J. Lauhon, in *Nature Nanotechnology*, 2008, **3**, pp. 168-173.

16. Z. W. Pan, Z. R. Dai and Z. L. Wang, *Science*, 2001, **291**, 1947-1949.

17. P. D. Yang, H. Q. Yan, S. Mao, R. Russo, J. Johnson, R. Saykally, N. Morris, J. Pham, R. R. He and H. J. Choi, *Advanced Functional Materials*, 2002, **12**, 323-331.

18. D. C. Look, *Materials Science and Engineering B-Solid State Materials for Advanced Technology*, 2001, **80**, 383-387.

19. M. E. Alf, A. Asatekin, M. C. Barr, S. H. Baxamusa, H. Chelawat, G. Ozaydin-Ince, C. D. Petruczok, R. Sreenivasan, W. E. Tenhaeff, N. J. Trujillo, S. Vaddiraju, J. J. Xu and K. K. Gleason, *Advanced Materials*, 2010, **22**, 1993-2027.

20. J. H. Park, C. C. Liu, M. K. Rathi, L. J. Mawst, P. F. Nealey and T. F. Kuech, *Journal of Nanophotonics*, 2009, **3**, 232-259

21. K. Angermaier and H. Schmidbaur, *Journal of the Chemical Society-Dalton Transactions*, 1995, **2** ,559-564.

22. C. C. Chen and C. C. Yeh, *Advanced Materials*, 2000, **12**, 738-739.

23. G. Z. Shen, P. C. Chen, Y. Bando, D. Golberg and C. W. Zhou, *Journal of Physical Chemistry C*, 2008, **112**, 16405-16410.

24. M. Q. He and S. N. Mohammad, *Journal of Vacuum Science & Technology B*, 2007, **25**, 940-944.

25. F. Kessler and D. Rudmann, *Solar Energy*, 2004, **77**, 685-695.

26. E. A. Stach, P. J. Pauzauskie, T. Kuykendall, J. Goldberger, R. R. He and P. D. Yang, *Nano Letters*, 2003, **3**, 867-869.

27. J. B. Hannon, S. Kodambaka, F. M. Ross and R. M. Tromp, *Nature*, 2006, **440**, 69-71.

28. J. P. Perdew, J. A. Chevary, S. H. Vosko, K. A. Jackson, M. R. Pederson, D. J. Singh and C. Fiolhais, *Physical Review B*, 1992, **46**, 6671-6687.

29. S. Fuke, Y. Takatsuka, K. Kuwahara and T. Imai, *Journal of Crystal Growth*, 1988, **87**, 567-570.

30. L. Brockway, M. Van Laer, S. Kohn and S. Vaddiraju, Unpublished manuscript.

31. F. Balzer, M. Schiek, H. G. Rubahn, K. Al-Shamery and A. Lutzen, *Journal of Vacuum Science & Technology B*, 2008, **26**, 1619-1623.

32. D. A. R. Barkhouse, A. G. Pattantyus-Abraham, L. Levina and E. H. Sargent, *Acs Nano*, 2008, **2**, 2356-2362.

33. H. Lim, C. Carraro, R. Maboudian, M. W. Pruessner and R. Ghodssi, *Langmuir*, 2004, **20**, 743-747.

34. F. Wang, H. Yu, J. Li, Q. Hang, D. Zemlyanov, P. C. Gibbons, L. W. Wang, D. B. Janes and W. E. Buhro, *Journal of the American Chemical Society*, 2007, **129**, 14327-14335.

35. G. M. Kimball, A. M. Muller, N. S. Lewis and H. A. Atwater, *Applied Physics Letters*, 2009, **95**.

36. F. J. Zong, H. L. Ma, J. Ma, W. Du, X. J. Zhang, H. D. Xiao, F. Ji and C. S. Xue, *Applied Physics Letters*, 2005, **87**.

37. G. Paniconi, Z. Stoeva, R. I. Smith, P. C. Dippo, B. L. Gallagher and D. H. Gregory, *Journal of Solid State Chemistry*, 2008, **181**, 158-165.

38. C. Pendyala, S. Vaddiraju, J. H. Kim, J. Jacinski, Z. Q. Chen and M. K. Sunkara, *Semiconductor Science and Technology*, 2010, **25**, 024014.

39. S. Vaddiraju, A. Mohite, A. Chin, M. Meyyappan, G. Sumanasekera, B. W. Alphenaar and M. K. Sunkara, *Nano Letters*, 2005, **5**, 1625-1631.

40. M. Green and P. O'Brien, *Chemistry of Materials*, 2001, **13**, 4500-4505.

41. B. Dimmler and R. Wachter, *Thin Solid Films*, 2007, **515**, 5973-5978.

42. M. A. Green, K. Emery, Y. Hishikawa and W. Warta, *Progress in Photovoltaics*, 2010, **18**, 346-352.

43. M. A. Green, K. Emery, Y. Hishikawa and W. Warta, *Progress in Photovoltaics: Research and Applications*, 2011, **19**, 84-92.

44. S.-S. Sun and N. S. Sariciftci, *Organic photovoltaics : mechanism, materials, and devices*, Taylor & Francis, Boca Raton, FL, 2005.

45. X. Gan, X. Li, X. Gao and W. Yu, *Journal of Alloys and Compounds*, 2009, **481**, 397-401.

CONTACT INFORMATION

Name:	Maxime Van Laer
Professional Address:	Dr. Sreeram Vaddiraju Department of Chemical Engineering BRWN 237 Texas A&M University College Station, TX 77843
Email Address:	maxvl_69@tamu.edu
Education:	B.A., Chemical Engineering, Texas A&M University December 2012 Omega Chi Epsilon Honors Society Dean's List Distinguished Student Undergraduate Research Scholar Research Fellow